

Ultrafast pulse characterization using cross phase modulation in silicon

En-Kuang Tien,^{a)} Xing-Zhu Sang, Feng Qing, Qi Song, and Ozdal Boyraz
Department of EECS, University of California, Irvine, California 92697, USA

(Received 15 May 2009; accepted 11 July 2009; published online 3 August 2009)

Based on the high nonlinearity of the chip-scale silicon waveguide with small dispersion, a compact frequency-resolved optical gating system has been demonstrated using cross phase modulation for ultrafast pulse characterization. The principal component generalized projections algorithm is used to retrieve the amplitude and phase from the spectrogram. Amplitude and phase of a 540 fs pulse have been measured. The measured amplitude result is confirmed by the autocorrelation measurement. © 2009 American Institute of Physics. [DOI: 10.1063/1.3193538]

The accurate amplitude and phase information of laser pulse is necessary to reveal the dynamic process in ultrafast applications. Although amplitude measurement is usually straightforward, the phase/chirp information of the pulse on time domain is not easy to be obtained from intensity measurements, and full characterization of ultrashort pulses is traditionally difficult. Self-reference methods, such as autocorrelation, spectral phase interferometry, and frequency-resolved optical gating (FROG), are invaluable tools to measure the pulse amplitude and phase of ultrashort laser pulses.¹⁻³ A FROG system is constructed by a second harmonic generation (SHG) autocorrelator followed by a spectrometer, and the amplitude and phase information can be extracted from single measurement. Other than using SHG, there are different “gating” mechanisms, which can be applied to FROG systems, such as polarization gating, self-diffraction, third harmonic generation, and cross phase modulation (XPM).¹ XPM FROG has been demonstrated as a good measurement tool⁴ in various nonlinear media, such as bulk silica and single mode fibers,⁵ microstructure optical fibers,⁶ and a quantum well structure device.⁷

Silicon has the inherent advantages of strong Kerr nonlinearity, which is more than 200 times higher than that of the silica glass. Additionally, the tight optical confinement due to large refractive index contrast between silicon core and silica cladding enhances the effective nonlinearity $\gamma = k_0 n_2 / A_{\text{eff}}$ by several orders of magnitude and facilitates large nonlinear phase shifting in short lengths. Self-phase modulation (SPM),⁸ XPM,⁹ and four wave mixing (FWM) (Ref. 10) have already been observed in silicon waveguides. Applications such as wavelength conversion, continuum generation, and ultrafast measurement using nonlinear effects in silicon have been demonstrated. In addition, two photon absorption (TPA) and TPA generated carriers are the dominant nonlinear absorption for wavelength from 1.1 to 2.2 μm .¹¹ In the application of ultrafast measurement, an autocorrelator has been demonstrated using two photon generated current in the silicon.¹² FWM has been utilized to demonstrate FROG measurement¹³ and an optical oscilloscope for pulsed lasers measurements.¹⁴

In this letter, we demonstrate a FROG system based on XPM in the silicon waveguide.¹⁵ Amplitude and phase measurement of a 540 fs mode-locked fiber lasers are experimentally presented. The measured results are confirmed by a two

photon current autocorrelation measurements using the same waveguide. Since enough nonlinear efficiency in silicon waveguides can be achieved in short length, dispersion can be engineered for short “walk off,” which facilitates precise pulse characterization at wavelengths from 1.2 to 5 μm without phase matching requirement.

Figure 1 illustrates the experimental setup used for silicon XPM FROG measurements. A fiber mode-locked laser at 1550 nm, which generates 540 fs pulses at 20 MHz repetition rate, is used as the source laser. The generated pulses then split into two paths by a polarization beam splitter (PBS). A polarization controller before splitting is inserted to control the splitting ratio and adjust the relative power levels of pump arm (also called the gate signal) and the probe arm. An optical time delay line constructed by two fiber collimators and a moving stage is used to produce tunable time delay for scanning. After passing the delay line, the two polarization branches are combined by a polarization beam coupler (PBC) and launched into a 1.7 cm silicon-on-insulator waveguide. The waveguide has 5 μm^2 modal area. A polarizer aligned with the probe pulse is used to filter the strong pump pulse and to facilitate measurement of changes on the probe arm. Then, we use an optical spectrum analyzer (OSA) to acquire the spectrum at each time delay and generate the spectrogram.

Since the dispersive effects are negligible, the propagated probe pulses will carry the information of nonlinear phase modulation, which can be defined as^{1,5}

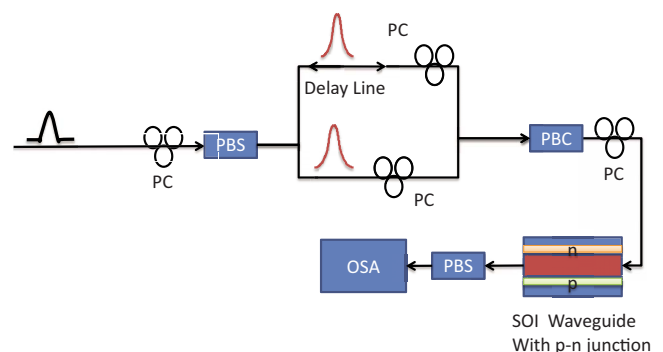


FIG. 1. (Color online) Schematic setup of XPM FROG in silicon. PC: polarization controller; PBS/PBC: polarization beam splitter/coupler; and OSA: optical spectrum analyzer.

^{a)}Electronic mail: etien@uci.edu.

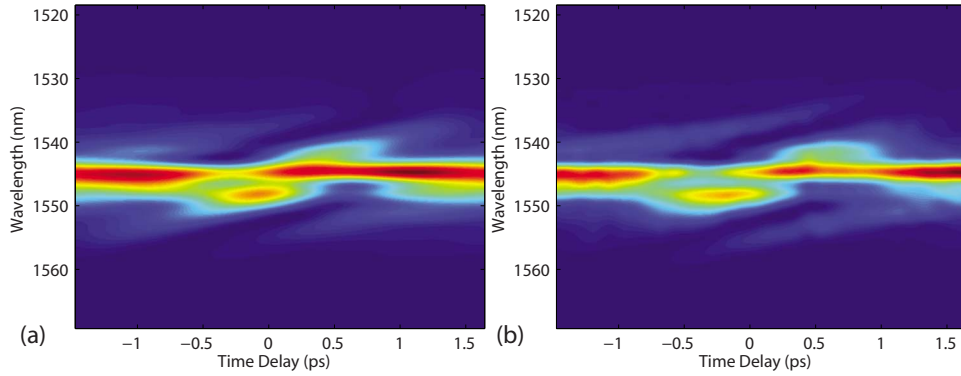


FIG. 2. (Color online) (a) Retrieved spectrogram and (b) measured spectrogram.

$$E_p^{\text{SPM+XPM}}(t, \tau) = E_{p0}(t) \exp\left(i\gamma L \left[\frac{2}{3}|E_p(t)|^2 + \frac{4}{3}|E_G(t-\tau)|^2\right]\right), \quad (1)$$

where $E_p(t)$ and $E_G(t)$ are probe and pump fields with orthogonal polarization states, γ is the Kerr nonlinear coefficient, and L is the length of the waveguide. The exponential term on the right hand side includes the nonlinear phase shift due to SPM and XPM.

However, by increasing the power in favor of the gate signal at the input, we can simplify Eq. (1) by neglecting the self phase modulation component as

$$E_{\text{sig}}^{\text{XPM}}(t, \tau) = E_p(t) e^{(4/3)i\gamma|E_G(t-\tau)|^2}. \quad (2)$$

The spectrum of the signal is

$$I_{\text{sig}}^{\text{XPM}}(\omega, \tau) = \left| \int_{-\infty}^{\infty} E_p(t) e^{(4/3)i\gamma|E_G(t-\tau)|^2} e^{i\omega t} dt \right|^2. \quad (3)$$

The spectrogram is generated by measuring the spectrum with respect to the delay between two signals. The pulse amplitude and phase information then can be retrieved from the spectrogram by using the principal component generalized projections (PCGPs) algorithm.¹⁶ In the PCGP algorithm some criteria of the probe and gate are required to avoid ambiguous solutions. For example, in SHG FROG the criteria are that the probe and gate fields are the same. In the XPM FROG, the probe field is the input probe field $E_p(t)$, and the gate function becomes the XPM exponential term $\exp(4/3i\gamma|E_G(t-\tau)|^2)$ in Fig. 2. Since the gate function is only a phase modulation on the probe pulse, the amplitude of the gate function is reset to one in each iteration while keeping the phase information from previous step. In addition, the spectrogram is filtered and normalized to compensate the energy fluctuations caused by TPA and the free carrier effect in silicon.

The sensitivity of the system can be estimated by assuming π phase shift generated from XPM within the waveguide. Given the nonlinear index of $n_2 = 6 \times 10^{-18} \text{ m}^2/\text{W}$, 25 W peak power is required for generate π phase shift in a 1.7 cm long waveguide with $5 \mu\text{m}^2$ mode area. It has been shown that pulse widths can be measure with XPM phase shift of 0.1 rad;⁵ thus the actual sensitivity of the experimental setup can be as low as 800 mW, which requires $31 \times$ lower power levels than what is required for π phase shift. The estimated sensitivity and dispersion limitation show that the system can be improved by using a silicon nanowire waveguide. For example, the waveguide dimension can be

reduced to $300 \times 500 \text{ nm}^2$ with good confinement. With the same peak power, the peak intensity in the nanowire will be ~ 30 times larger than inside a $5 \mu\text{m}^2$ waveguide, and the power requirement to achieve the same nonlinear phase shift can be decreased by a factor of 30. We also would like to highlight that short pulse measurements in XPM FROG usually require low power levels to induce $< \pi$ phase shift, and hence the free carrier contribution on the phase shift is negligible. Furthermore, the free carrier lifetime in a nanowire is much shorter than that of large waveguides, and free carrier dispersion and absorption effect will be reduced further.

The spectrogram for measurement of a femtosecond pulse generated from the mode-locked fiber laser is shown in Fig. 2(a). The spectrogram is taken within 3 ps time delay. The input pulse is then retrieved by the PCGP algorithm. Figure 2(b) shows that the error between the measured and retrieved spectrograms is 0.03%, which can be attributed to imperfections in the polarization combining and irregularities in manual scanning. After > 5000 iterations, the actual pulse amplitude and phase information are generated. The retrieved pulse and the phase are shown in Fig. 3. We can see that the input pulse has a full width half maximum width of 540 fs. Given the 0.5 mW average power of the laser, the peak power of the pulse can be estimated to be $\sim 46 \text{ W}$. The structure of the pedestal of the pulse is also reconstructed and resolved by the FROG system. To confirm the measurement, an autocorrelation measurement is performed by measuring the TPA generated current across the p - n junction over the waveguide with respect to the time delay between two arms of the probe and gate pulses.¹² Figure 4 shows the pulse measured by XPM FROG with pulse measured by autocor-

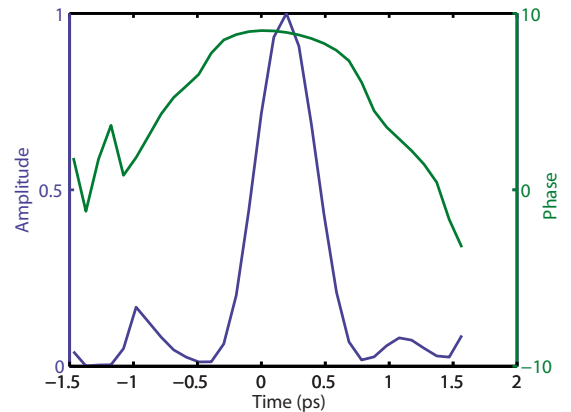


FIG. 3. (Color online) Retrieved pulse and phase.

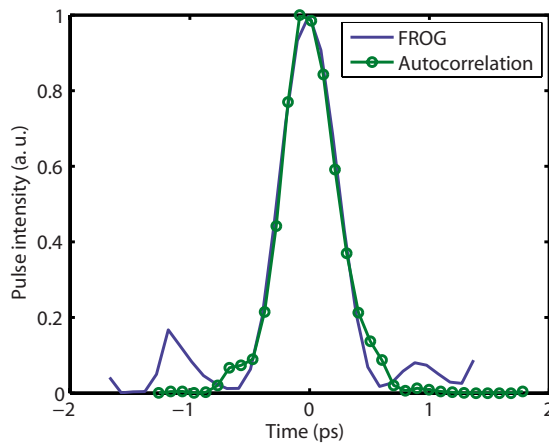


FIG. 4. (Color online) FROG measured pulse and the autocorrelator measured pulse.

relation. As expected we achieve good agreement on the pulse envelope with the exception of lost sharp features in the autocorrelation measurements as illustrated by the red curve in Fig. 4. We also would like to highlight that the dispersion within the waveguide will limit the minimum measurable pulse durations in XPM FROG systems.⁵ The dispersion can be ignored when pulse duration is longer than $T_{o,min} = (20|\beta_2|L)^{0.5}$. Assuming that dispersion is mainly determined by material dispersion, we estimate that the minimum measurable pulse width in a 1.7 cm long waveguide is $T_{o,min} = 500$ fs. Another advantage of using a silicon nanowire is that waveguide dispersion can be adjusted by changing the waveguide dimension to be close to zero at a designate wavelength.¹⁷ Thus the group velocity dispersion inside the waveguide can be ignored at the wavelength to achieve short pulse measurement.

In summary, a compact FROG system for measuring the pulse amplitude and phase of ultrafast pulses has been demonstrated by XPM in silicon. Amplitude and phase measurement of a 540 fs pulse are experimentally and successfully carried out by this system. The amplitude result is compared with that of an autocorrelation measurement, which shows good agreement.

Because of the short length and the small dispersion induced walk off, silicon based XPM FROG can be used for precise ultrafast pulse characterization at wavelengths from 1.2 μm to midinfrared wavelengths without phase matching requirement. In addition, since the optical intensity in the waveguide is depend on the size of model area, the sensitivity can be improved by using a silicon nanowires.

¹R. Trebino, *Frequency-Resolved Optical Gating: The Measurement of Ultrashort Laser Pulses* (Kluwer, Norwell, MA, 2002).

²K. F. Lee, K. J. Kubarych, A. Bonvalet, and M. Joffe, *J. Opt. Soc. Am. B* **25**, A54 (2008).

³C. Dorrer and I. Kang, *J. Opt. Soc. Am. B* **25**, A1 (2008).

⁴M. A. Franco, H. R. Lange, J. F. Ripoche, B. S. Prade, and A. Mysyrowicz, *Opt. Commun.* **140**, 331 (1997).

⁵M. D. Thomson, J. M. Dudley, L. P. Barry, and J. D. Harvey, *Opt. Lett.* **23**, 1582 (1998).

⁶J. Dudley, X. Gu, L. Xu, M. Kimmel, E. Zeek, P. O'Shea, R. Trebino, S. Coen, and R. Windeler, *Opt. Express* **10**, 1215 (2002). <http://opticsinfobase.org/oe/abstract.cfm?uri=OE-10-21-1215>.

⁷D. Reid, P. J. Maguire, L. P. Barry, Q.-T. Le, S. Lobo, M. Gay, L. Bramerie, M. Joindot, Jean-Claude Simon, D. Massoubre, Jean-Louis Oudar, and Guy Aubin, *J. Opt. Soc. Am. B* **25**, A133 (2008).

⁸E. Dulkeith, Y. A. Vlasov, X. G. Chen, N. C. Panoiu, and R. M. Osgood, *Opt. Express* **14**, 5524 (2006).

⁹I. W. Hsieh, X. G. Chen, J. I. Dadap, N. C. Panoiu, R. M. Osgood, S. J. McNab, and Y. A. Vlasov, *Opt. Express* **15**, 1135 (2007).

¹⁰H. Fukuda, K. Yamada, T. Shoji, M. Takahashi, T. Tsuchizawa, T. Watanabe, J. Takahashi, and S. Itabashi, *Opt. Express* **13**, 4629 (2005).

¹¹E.-K. Tien, F. Qian, N. S. Yuksek, and O. Boyraz, *Appl. Phys. Lett.* **91**, 201115 (2007).

¹²T. K. Liang, H. K. Tsang, I. E. Day, J. Drake, A. P. Knights, and M. Asghari, *Appl. Phys. Lett.* **81**, 1323 (2002).

¹³M. A. Foster, R. Salem, D. F. Geraghty, A. C. Turner-Foster, M. Lipson, and A. L. Gaeta, presented at the Coherent Optical Technologies and Applications, 2008 (unpublished). <http://www.opticsinfobase.org/abstract.cfm?URI=COTA-2008-CMC4>.

¹⁴M. A. Foster, R. Salem, D. F. Geraghty, A. C. Turner-Foster, M. Lipson, and A. L. Gaeta, *Nature (London)* **456**, 81 (2008).

¹⁵E. K. Tien, X.-Z. Sang, F. Qing, Q. Song, and O. Boyraz, presented at the 21st Annual Meeting of the IEEE Lasers and Electro-Optics Society, 2008 (LEOS 2008) (unpublished). http://www.ieeeexplore.ieee.org/xpls/abs_all.jsp?isnumber=4688450&arnumber=4688612&count=462&index=160.

¹⁶D. J. Kane, *IEEE J. Sel. Top. Quantum Electron.* **4**, 278 (1998).

¹⁷Q. Lin, J. D. Zhang, P. M. Fauchet, and G. P. Agrawal, *Opt. Express* **14**, 4786 (2006).